Biology and Fertility of Soils (2022) 58:707–720
https://doi.org/10.1007/s00374-022-01653-w

ORIGINAL PAPER

Topography-driven soil properties modulate effects of nitrogen deposition on soil nitrous oxide sources in a subtropical forest

Pengpeng Duan[1,2] · Xinyi Yang[1,2] · Xunyang He[1,2] · Yonglei Jiang[3] · Kongcao Xiao[1,2] · Kelin Wang[1,2] · Dejun Li[1,2]

Received: 15 February 2022 / Revised: 5 July 2022 / Accepted: 8 July 2022 / Published online: 30 July 2022

Abstract

An ex-situ ^{15}N–^{18}O tracing experiment with soils collected from the valley and slope, respectively, of a subtropical secondary karst forest with three N addition levels, i.e., 0, 50, and 100 kg N ha^{-1} $year^{-1}$ for each topographic position to investigate N_2O production pathways. Autotrophic nitrification pathways (ammonia oxidation, nitrifier denitrification, and nitrification-coupled denitrification) accounted for > 70% of total N_2O production, but denitrification pathways (heterotrophic denitrification and co-denitrification) were the minor source of N_2O at both topographic positions. In the valley, chronic N addition stimulated ammonia oxidation-derived N_2O, which was paralleled by increased ammonia-oxidizing archaea (AOA) *amoA* gene transcript abundance, but inhibited nitrifier denitrification- and nitrification-coupled denitrification–derived N_2O along with suppressed ammonia-oxidizing bacteria (AOB) *amoA* gene transcript abundance and stimulated *nosZ*II gene transcript abundance, respectively. On the slope, chronic N addition stimulated ammonia oxidation-derived N_2O along with increased AOB *amoA* gene transcript abundance, and enhanced nitrifier denitrification-derived N_2O congruent with increased AOB *amoA* and decreased *nirK* gene transcript abundances. In addition, chronic N addition reduced the relative contribution of heterotrophic denitrification to N_2O production but had no significant influence on heterotrophic denitrification-derived N_2O on the slope. Overall, our results provide a comprehensive view in terms of how topography-driven soil properties regulate N_2O production and its pathways in a subtropical forest.

Keywords N deposition · Topography · Ammonia oxidation · Nitrifier denitrification · Nitrification-coupled denitrification · Heterotrophic denitrification · Transcripts

Introduction

Soils are the predominant source of atmospheric nitrous oxide (N_2O) (Tian et al. 2020), which is a potent greenhouse gas and long-lived stratospheric ozone-depleting substance (Montzka et al. 2011). Soil N_2O emission from natural ecosystems has been increasing with a rate of 0.7 ± 0.5 Tg N $year^{-1}$ since the 1860s, and accounted for 67% of global soil N_2O emission during the period from 2007 to 2016 (Tian et al. 2019a). Nevertheless, the increase in soil N_2O emission is region-specific. For example, soil N_2O emission from natural ecosystems in China has increased from 0.3 ± 0.1 Tg N $year^{-1}$ in the 1860s to 0.5 ± 0.5 Tg N $year^{-1}$ for the period from 2007 to 2016 largely due to atmospheric nitrogen (N) deposition; but soil N_2O emission from natural ecosystems in the USA is relatively constant over the same time scale (Tian et al. 2019a). Considering the huge uncertainty in the simulation of soil N_2O emission by process-based terrestrial biosphere models, it is hence imperative to unravel the mechanisms underlying the change of soil N_2O production in response to atmospheric N deposition.

Nitrification and denitrification are the predominant microbial processes that produce N_2O in soil (Butterbach-Bahl et al. 2013). Nitrification pathways include ammonia oxidation (Prosser et al. 2020), heterotrophic nitrification (Zhang et al. 2015), nitrifier denitrification (Wrage-Mönnig

✉ Dejun Li
dejunli@isa.ac.cn; lidejun@hotmail.com

1 Guangxi Key Laboratory of Karst Ecological Processes and Services, Huanjiang Observation and Research Station for Karst Ecosystems, Institute of Subtropical Agriculture, Chinese Academy of Sciences, Huanjiang 547100, China

2 Key Laboratory of Agro–Ecological Processes in Subtropical Region, Institute of Subtropical Agriculture, Chinese Academy of Sciences, Changsha 410125, China

3 Yunnan Academy of Tobacco Agricultural Sciences, Kunming 650021, China

et al. 2018), and nitrification-coupled denitrification (Verhoeven et al. 2018). During nitrification, N_2O production is regulated by *amoA* gene encoding the ammonia monooxygenase enzyme of ammonia-oxidizing archaea (AOA), ammonia-oxidizing bacteria (AOB), and complete ammonia-oxidizing bacteria (comammox) (Li et al. 2022). Denitrification pathways include heterotrophic denitrification, codenitrification (Spott et al. 2011), and chemodenitrification (Chalk and Smith 2020). The key step of denitrification is the reduction of nitrite into nitric oxide catalyzed by nitrite reductase encoded by *nirK*, *nirS* (Clark et al. 2012). or fungal *nirK* gene (Aldossari and Ishii 2021). The last step of bacterial denitrification is catalyzed by N_2O reductase encoded by *nosZI* and/or *nosZII* genes (Hallin et al. 2018), which is the only known sink of N_2O in the biosphere, as it reduces N_2O into N_2 under conditions of oxygen limitation and high carbon (C) availability (Fig. S2) (Duan et al. 2019b; Krause et al. 2017). As nitrifier and denitrifier activities are sensitive to substrate availability (Hallin et al. 2018; Prosser et al. 2020), N addition could affect nitrification and denitrification and thus soil N_2O production, which was closely linked to the relative abundance of microbial functional genes involved in nitrification and denitrification in tropical/subtropical forests, but the potential mechanism was rarely explored (Han et al. 2019; Song et al. 2020; Soper et al. 2018; Tian et al. 2019b). While previous studies have simultaneously measured nitrification and heterotrophic denitrification in forest soil and used these processes to explain the change of soil N_2O production under elevated N deposition (Han et al. 2018b; Peng et al. 2021; Tang et al. 2018), it remains challenging to distinguish the contribution of other processes, e.g., nitrifier denitrification and nitrification-coupled denitrification to soil N_2O production.

Besides soil N availability, the other soil properties, such as soil organic C (SOC) has often been found to affect the responses of soil N_2O emission to N addition (Tian et al. 2019b; Wu et al. 2020; Yan et al. 2018). For example, N addition significantly increased soil N_2O emission by stimulating the abundances of denitrifiers due to high SOC availability (Han et al. 2018b). Topographic position has been identified as a major determinant for soil properties, soil N transformation rates, soil microbial community composition, and abundance, etc., which may subsequently affect N_2O emission (Arias-Navarro et al. 2017; Stewart et al. 2014; Zhu et al. 2021). Relative to the slope, soils in the valley are often characterized by greater levels of dissolved organic C (DOC) and NO_3^-, higher moisture, and more O_2 depletion, which favor the formation of hot spots for N_2O production via denitrification (Stewart et al. 2014; Zhu et al. 2021). Nevertheless, it has never been investigated, to our knowledge, whether and how the effects of N addition on the contribution of multiple pathways of N_2O production are modulated by topography.

To elucidate the soil N transformation and N_2O production pathways and their responses to N addition, we conducted an ex situ ^{15}N–^{18}O tracing experiment with soils collected from the valley and slope of a subtropical karst forest after 3 years of N addition in southwest China. Paired ($^{15}NH_4^+$–$^{15}NO_3^-$) and dual (^{15}N–^{18}O) isotope labeling techniques (Jansen-Willems et al. 2016; Kool et al. 2011) combined with mathematical modelling were used to differentiate seven N_2O production pathways (Fig. S2). Transcriptional analyses of key microbial functional genes were performed to link the changes in the expression of functional genes with soil N_2O production through different pathways. Our previous studies show that the calcareous soils in this region have high soil acid buffering capacity due to high contents of calcium (Ca) and magnesium (Mg) (Wang et al. 2019; Zheng et al. 2020). Since enhanced N deposition can promote nitrification in calcareous soil without acidification (Hao et al. 2020), we hypothesized that N addition would increase the contribution of nitrification to N_2O production because of rapid utilization of NH_4^+ from N addition (Hypothesis I). In two companion studies, we reported that SOC content was higher on the slope than in the valley, while NO_3^- availability was higher in the valley than on the slope (Chen et al. 2021; Wang et al. 2019). Since N_2O reduction via denitrification depends on NO_3^- and SOC content, with higher NO_3^- but lower SOC content inhibiting activity of N_2O-reducing microorganisms (Hallin et al. 2018), we hypothesized that N addition would increase the contribution of denitrification to N_2O production in the valley due to the higher soil NO_3^- but lower C level (Hypothesis II).

Materials and methods

Site description and experimental design

The N addition experiment was conducted in Mulun National Nature Reserve of Huanjiang County, southwest China (Wang et al. 2019). The region has a humid subtropical climate. Mean annual precipitation and air temperature are 1389 mm and 19 °C, respectively. Atmospheric N deposition rate was approximately 37 kg N ha^{-1} $year^{-1}$ according to Zhu et al. (2015).

The experiment was conducted at two topographic positions, i.e., in the valley and on the slope, respectively, of a secondary karst forest. The soil, underlain by limestone, is classified as leptosols (limestone soil) according to World Reference Base classification system. Soil depth in the valley and on the slope varies from 0.0 to 0.8 m and from 0.0 to 0.3 m, respectively. The distance between the neighboring plots of the two topographic positions is greater than 30 m. There are lots of fissures and small conduits in the limestone underlain the karst ecosystems, so that the

hydrological process is dominated by vertical leakage via the fissures and small conduits instead of overland flow or interflow (Fu et al. 2016). The selected forest is about 35 years old after clear-cut, and dominated by *Cryptocar yachinensis* (Hance) Hemsl., *Cinnamomum saxatile* H.W.Li, *Koelreuteria minor* Hemsl., *Pittosporum tobira* (Thunb.) Ait., *Bridelia tomentosa* Bl., and *Murraya exotica* L. Mant. The basal area of trees is 229.6 ± 65.3 (mean ± standard deviation) m^2 ha^{-1} in the valley and 195.5 ± 71.4 m^2 ha^{-1} on the slope. At each position, a randomized complete block design was applied with three blocks and three N addition levels, i.e., control (N0, 0 kg N ha^{-1} $year^{-1}$), moderate N addition (N50, 50 kg N ha^{-1} $year^{-1}$), and high N addition (N100, 100 kg N ha^{-1} $year^{-1}$). Therefore, there are nine plots (10 × 10 m each) at each topographic position (Fig. S1). Each plot was surrounded by a 10-m wide buffering zone to avoid potential influence from each other. Nitrogen was applied in the form of NH_4NO_3 at the beginning of each month since April 2016. On each N addition event, NH_4NO_3 was dissolved in 10 L of water (equal to 1.2 mm extra mm precipitation per year) and sprayed with a back–pack sprayer. The control plots received an equal amount of water.

Soil physicochemical properties

Ten soil samples were taken randomly using a soil corer (5 cm in inner diameter) from the mineral soil horizon to a depth of 0–10 cm, and mixed thoroughly to a composite sample for each plot in September 24, 2019. In total, > 1.5-kg composite sample was collected from each plot. The soil samples were stored in zip-locked polypropylene bags and placed in a cool box during transportation to the laboratory. After carefully removing the litter, roots, and stones by hand with a tweezers, each composite soil sample was passed through a 2-mm sieve, and was divided into four subsamples. One fresh subsample was stored at − 20 °C and used for the DNA extraction. One fresh subsample was stored at 4 °C and used to determine DOC, total dissolved N (TDN), NH_4^+, NO_2^-, NO_3^-, available P (AVP), microbial biomass C (MBC), N (MBN), and P (MBP) within 1 week. One fresh subsample was stored at 4 °C and used for the incubation experiment in October 2019. One subsample was air dried, sieved to 1 mm, and used to determine pH, exchangeable Ca and Mg, soil organic C (SOC), total N (TN), and total P (TP). Methods for the physicochemical analyses are presented in detail in Carter and Gregorich (2007). Soil moisture content was measured by weighting and drying for 24 h at 105 °C. Soil exchangeable Ca and Mg were analyzed by an inductively coupled plasma atomic emission spectroscopy (ICP-AES). Soil pH (1:2.5 soil/water ratio) was measured with a pH meter (FE20K, Mettler-Toledo, Switzerland). SOC was measured by dichromate redox colorimetric method. TN were analyzed using an elemental analyzer (EA 3000; EuroVector, Italy). TP were analyzed colorimetrically using ascorbic acid molybdate method. DOC and TDN were measured by the wet oxidation and persulfate oxidation methods, respectively. Exchangeable NH_4^+ and NO_3^- were analyzed by an auto-analyzer (FIAstar 5000, FOSS, Sweden). AVP were measured using the molybdenum blue colorimetric method. MBC, MBN, and MBP were measured using chloroform fumigation–extraction method (Brookes et al. 1985; Vance et al. 1987). The above variables are presented in Table S3.

Soil microcosm experiment

Soils were stored in a refrigerator (4 °C) before starting the incubation experiment in October 2019. Two sets of microcosm experiments were carried out. The first experiment aimed to evaluate whether abiotic N_2O production played an important role or not (See Supplemental Methods for details). The second experiment aimed to determine N_2O production from multiple microbial processes. According to the first experiment, abiotic N_2O production was negligible, so that only the second experiment is presented below.

Soil samples were pre-incubated at 50% water holding capacity (WHC) and 20 °C for 7 days in 120-ml serum bottles, each of which was loaded with 10-g soil (dry weight equivalent). Upon pre-incubation, soil samples from each plot received with four treatments, i.e., (a) ^{18}O-H_2O + NO_3^- + NH_4^+, (b) H_2O + ^{18}O-NO_3^- + NH_4^+, (c) H_2O + ^{15} N-NO_3^- + NH_4^+, and (d) H_2O + NO_3^- + ^{15} N–NH_4^+. In total, the laboratory experiment had 216 serum vials [2 topographic positions × 3 N addition levels × 3 blocks × 6 isotope treatments (2 sampling times for ^{15} N labeled + 1 sampling times for ^{15} N and ^{18}O labeled) × 2 replicates]. All the microcosms received NH_4NO_3 at a rate of 50.0 mg N kg^{-1} soil (25 mg NH_4^+–N kg^{-1} and 25 mg NO_3^-–N kg^{-1} soil), which was equivalent to an atmospheric N deposition rate of 40 kg N ha^{-1} $year^{-1}$ in southwest of China (Wen et al. 2020). ^{18}O and ^{15} N were enriched to a final abundance of 1.0 atom% ^{18}O and 10.0 atom% ^{15} N excess, respectively. After ^{18}O and ^{15} N addition, the microcosms were adjusted at 60% WHC, serum bottles were tightly capped with aluminum caps, and incubated for 36 h at 20 °C.

It should be noted that the incubation conditions of moisture and temperature were identified based on the following three aspects. First, the WHC condition was chosen since it was reported to be optimum for the simultaneous occurrence of nitrification and denitrification (Congreves et al. 2019) due to the uninhibited diffusion of both substrates and O_2 (Parton et al. 1996) and the occurrence of anaerobic microsites in soil aggregates (Sexstone et al. 1985). Second, this region is located in the subtropical humid forest life zone with a monsoon climate. The mean annual air temperature

ranges from 17.8 to 22.2 °C in Huanjiang County, and mean soil temperature ranges from 18.8 to 20.1 °C in the N addition experiment, thus we used the average (20 °C) as the incubation temperature in the current study.

At the end of incubation, 50-ml headspace gas was collected from each bottle and evenly injected into two 12-ml pre-evacuated glass vials (Labco Exetainer, Labco Limited, UK). One gas sample was used for $^{15}N_2O$, $N_2{}^{18}O$, $^{29}N_2$, and $^{30}N_2$ analyses using a MAT 253 isotope ratio mass spectrometer (Thermo Finnigan MAT, Bremen, Germany). The m/z 29 and 30 beams enabled calculation of molecular ratios of ^{29}R ($^{29}N_2/^{28}N_2$) and ^{30}R ($^{30}N_2/^{28}N_2$) for N_2 (Yang et al. 2014). Based on the $^{15}N_2$ data, none of the ^{15} N-labeled N_2O was further reduced to N_2 (data not shown). Another gas sample was used for the analyses of N_2O and CO_2 concentrations using a gas chromatograph (Agilent 7890A, Agilent Ltd., CA, USA).

The headspace gas was sampled 30 min after the tracer addition, and soils in treatments (c) and (d) were extracted with 2 M KCl (soil:KCl = 1:5) to determine the concentrations and ^{15} N abundance of NO_3^- and NH_4^+. An auto-analyzer (FIAstar 5,000, FOSS, Sweden) was used to analyze NO_3^- and NH_4^+ concentrations. ^{15} N analysis was performed after chemically transforming NO_3^- and NH_4^+ to N_2O (Laughlin et al. 1997; Liu et al. 2014; Stevens and Laughlin 1994) using a MAT 253 isotope–ratio mass spectrometer (Thermo Finnigan MAT, Bremen, Germany). After extraction, soils were washed with distilled water for three times (Duan et al. 2019c; Peng et al. 2021; Zhang et al. 2018b), and then dried at 60 °C and used for the analyses of ^{15} N abundance of organic N using a MAT 253 isotope–ratio mass spectrometer coupled with an FLASH2000HT elemental analyzer (Thermo Finnigan MAT, Bremen, Germany).

At the end of incubation, soils in treatments (a) and (b) were used to extract RNA, which was further used to measure transcript abundances of nitrification and denitrification genes. According to the manufacturer's instructions, 2.0-g fresh soil was used to extract RNA using a Power Soil Total RNA Isolation Kit (MO BIO Laboratories, Carlsbad, USA) (Duan et al. 2019a). RNA was quantified spectrophotometrically (NanoDrop Technologies Inc., Wilmington, DE, USA). The RNA extracts were treated with a DNase I kit (MO BIO Laboratories, Carlsbad, CA, USA) to remove DNA residuals. RNA was transcribed into complementary DNA (cDNA) using RT Easy™ I (World's Foregene, China) for first-strand cDNA synthesis. The purified cDNA samples were stored at − 20 °C until further analysis.

RT-qPCR was used to measure the abundances of two ammonia monooxygenases (AOA *amoA* and AOB *amoA*) and five denitrification reductases (*nirK*, *nirS*, fungal *nirK*, *nosZ*I, and *nosZ*II). RT-qPCR primers are described in Table S1. Each RT-qPCR reaction mixtures contained 1 µl of template cDNA or serially diluted standards, 5 µl of SYBR Premix Ex Taq II (TaKaRa Biotechnology, Otsu, Shiga, Japan), 0.2 µl each of forward and reverse primer, 0.2 µl of ROX Reference Dye I, and 3.6 µl of RNAase/DNase-free water. Standards ranging from 10^8 to 10^1 gene copies μL^{-1} were prepared from linearized plasmids with insertions of target gene fragments. The amplification efficiencies ranged between 89.5 and 94.3%, and R^2 values were > 0.98 for all the genes.

Calculations and statistical analysis

Gross mineralization (GMR) and nitrification rates (GNR) were calculated as described before (Davidson et al. 1991; Li et al. 2018). A mathematical model named "pool mixing model" was used to quantify the relative contributions of four pathways to N_2O production, based on the Excel Solver method (Duan et al. 2019c; Jansen-Willems et al. 2016). Three assumptions for this model are: (i) N_2O comes from three uniformly distributed pools; (ii) four processes are taken into account, i.e., autotrophic nitrification (AN), heterotrophic nitrification (HN), co-denitrification (CD), and heterotrophic denitrification (HD); and (iii) isotopic discrimination is considered to be negligible. The three uniformly distributed pools are NH_4^+, organic N, and NO_3^- pools, respectively. N_2O derived from the NH_4^+ pool via autotrophic nitrification at enrichment a_n, from organic N pool via heterotrophic nitrification at enrichment a_o, and from NO_3^- pool via denitrification at enrichment a_d. Co-denitrification defined as the hybrid formation of N_2O, which is formed by one N atom from the NO_3^- pool and one from the organic N pool. The detailed derivations for this model are provided in Supplemental Methods (Eqs. (1)–(9)).

A dual-isotope (^{15} N–^{18}O) labeling approach was used to distinguish the contribution of nitrification pathways (ammonia oxidation—AO, nitrifier denitrification—ND, and nitrification-coupled denitrification—NCD) and HD to N_2O production (Kool et al. 2011). The main assumptions underlying this approach are: (i) ammonia oxidation-derived N_2O does not contain any O from H_2O; (ii) NO_3^- is the substrate for heterotrophic denitrification and an obligatory intermediate for nitrification-coupled denitrification; (iii) O exchange takes place at the same rate as quantified for denitrification from NO_3^- to N_2O across these pathways; (iv) O atom originates from H_2O, O_2, and NO_3^- in ratios reflecting the reaction stoichiometry for AO, ND, NCD, and HD (Table S2). The detailed calculations are provided in Supplemental Methods (Eqs. (10)–(29)).

Following the hole-in-the-pipe model, the fraction (R) of N_2O lost via nitrification was calculated using Eq. (1):

$$RN_2O_{AN/AO/ND} = \frac{N_2O_{AN/AO/ND}}{GNR} \quad (1)$$

where $N_2O_{AN/AO/ND}$ denotes N_2O produced by autotrophic nitrification or ammonia oxidation or nitrifier denitrification.

Note that autotrophic nitrification may include ammonia oxidation and nitrifier denitrification when using pool-mixing model. Therefore, we distinguished ammonia oxidation from autotrophic nitrification.

Statistical analysis

Two-way analysis of variance (ANOVA) with least significant difference (LSD) test was adopted to examine the effects of field N addition, topography and their interaction on net N_2O production, contribution of individual pathways to net N_2O production, and functional gene transcript abundances. One-way ANOVA with LSD test was used to examine the effects of field N addition on net N_2O production, contribution of individual pathways to total N_2O production, and functional gene transcript abundances either in the valley or on the slope. Independent samples *t* test was used to examine whether the difference is significant between the two topographic positions for the same field N addition level. The effect was considered significant at $p < 0.05$ level. The above analyses were performed in SPSS 20.0 (IBM Co., Armonk, NY, USA). To test the relationships among N_2O production pathways, soil properties, and functional gene transcript abundances, we adopted Pearson correlation analysis using the R packages *ggm* and *psych* (R version 3.3.1).

Structural equation modelling (SEM) was performed to partition the direct and indirect effects of soil properties and functional gene transcripts on N_2O production rate from individual pathways (expressed as pathway-derived N_2O) in the valley and on the slope. The hypothesized model was considered to fit the data well if the chi-square test is not significant ($p > 0.05$), and was rejected if the chi-square test was significant ($p < 0.05$). The SEM analyses were conducted using AMOS 21.0 (Amos Development Corporation, Chicago, IL, USA).

Results

Soil N_2O production and its contributions from different pathways

Significant interactive effects of topography × N addition on net N_2O production, contribution of autotrophic nitrification, nitrifier denitrification, nitrification-coupled denitrification, and heterotrophic denitrification to N_2O production were found (Table S4). Net N_2O production during the laboratory incubation experiment was significantly ($p < 0.05$) greater for soils under chronic 3-year high N addition regardless of topographic position (Fig. 1a). Net N_2O production was significantly higher ($p < 0.05$) for soils collected from the slope than from the valley under N100 (Fig. 1a). Autotrophic nitrification was the main source of N_2O by accounting for 93.1 ± 2.8–96.4 ± 0.6% in the valley and 87.9 ± 0.6–95.9 ± 0.8% on the slope of the total N_2O production (Fig. 1b). Chronic N addition significantly ($p < 0.05$) increased the contribution of autotrophic nitrification to N_2O production on the slope, but not in the valley (Fig. 1b).

The N_2O production rate by autotrophic nitrification was significantly ($p < 0.05$) increased at both topographic positions by N addition (Table 1). Heterotrophic denitrification was responsible for 3.6 ± 0.6–5.9 ± 2.8% in the valley and

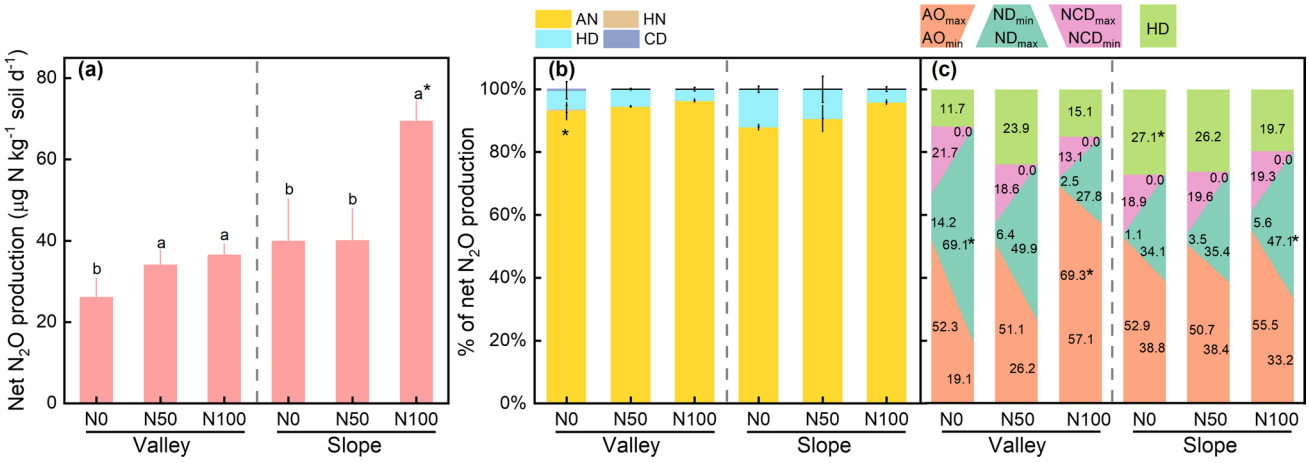

Fig. 1 Impacts of N addition on (**a**) total N_2O production, and relative contributions of N_2O production pathways in the valley and on the slope either (**b**) based on a pool mixing model, or (**c**) based on a dual–isotope labeling approach. Different letters denote significant difference at $p < 0.05$ among N addition treatments in the valley or on the slope. The asterisk (*) indicates significant difference at $p < 0.05$ between the valley and slope for the same N addition level. Values are presented as means with standard deviations ($n = 3$). AN, autotrophic nitrification; HN, heterotrophic nitrification; HD, heterotrophic denitrification; CD, co-denitrification; AO, ammonia oxidation; ND, nitrifier denitrification; NCD, nitrification-coupled denitrification

4.1 ± 0.8–12.0 ± 1.0% on the slope of the total N_2O production. Chronic N addition significantly ($p < 0.05$) decreased the contribution of heterotrophic denitrification to N_2O production on the slope but not in the valley (Fig. 1b). However, there was no significant influence of N addition on N_2O production rate from heterotrophic denitrification at both topographic positions (Table 1). The contributions of heterotrophic nitrification and co-denitrification to total N_2O production were negligible and not significantly different among the N addition treatments (Fig. 1b).

The contribution of ammonia oxidation to N_2O production ranged from minima of 19.1 ± 6.5 to maxima of 52.3 ± 5.0% in the valley and from minima of 38.8 ± 6.9 to maxima of 52.9 ± 6.3% on the slope under the control (Fig. 1c). The contribution of nitrifier denitrification to N_2O production ranged from minima of 14.2 ± 0.9 to maxima of 69.1 ± 3.1% in the valley and from minima of 1.1 ± 0.9 to maxima of 34.1 ± 5.2% on the slope under the control. Nitrification-coupled denitrification contributed 21.7 ± 1.0% in the valley and 18.9 ± 5.7% on the slope to N_2O production under the control. Heterotrophic denitrification contributed 11.7 ± 6.1% in the valley and 27.1 ± 1.7% on the slope to N_2O production under the control. Chronic N addition significantly ($p < 0.05$) increased the contribution of ammonia oxidation, while significantly ($p < 0.05$) decreased the contribution of nitrifier denitrification and nitrification-coupled denitrification to N_2O production in the valley. The N_2O production rate from ammonia oxidation was significantly increased, but that was decreased from nitrifier denitrification in the valley by N addition (Table 1). Chronic N addition significantly ($p < 0.05$) increased the contribution of nitrifier denitrification to N_2O production and N_2O production rate from ammonia oxidation and nitrifier denitrification on the slope (Table 1).

Microbial transcript abundances

Significant interactive effect of topography × N addition on AOB *amoA* and *nosZ*I transcripts was found (Table S4). Compared to the control, AOB *amoA* transcript was significantly ($p < 0.05$) decreased in the valley whereas increased on the slope under chronic N addition (Fig. 2b). AOA:AOB *amoA* ratio was significantly ($p < 0.05$) increased by chronic N addition in the valley (Fig. 2c). AOB *amoA* transcript was significantly higher ($p < 0.05$) in the valley than on the slope for the control, while the ratio of AOA:AOB *amoA* was significantly higher ($p < 0.05$) on the slope than in the valley only for the control (Fig. 2b, c). In addition, AOB *amoA* transcript was significantly higher on the slope than in the valley under N100.

Chronic N addition significantly ($p < 0.05$) decreased *nirK* transcript relative to the control at the two topographic

Table 1 Effects of N addition on the amount of N_2O derived from different biological pathways, gross N mineralization and nitrification rates, and the fraction of gross nitrification rate emitted as N_2O in the valley and on the slope. Values are means ± standard deviations ($n = 3$)

	Valley			Slope		
Processes	**N0**	**N50**	**N100**	**N0**	**N50**	**N100**
Autotrophic nitrification (μg N kg d^{-1})	24.1 ± 4b	32.2 ± 3.6a	35.1 ± 2.7a	35 ± 9.6b	36.1 ± 6.3b	66.5 ± 4.6a*
Heterotrophic nitrification (μg N kg d^{-1})	0.2 ± 0.4a	0 ± 0a	0 ± 0a	0 ± 0a	0 ± 0a	0 ± 0a
Heterotrophic denitrification (μg N kg d^{-1})	1.6 ± 0.8a	1.9 ± 0.1a	1.3 ± 0.2a	4.7 ± 1.1a*	3.9 ± 2.2a	2.9 ± 0.7a
Co–denitrification (μg N kg d^{-1})	0.1 ± 0.1a	0 ± 0a	0 ± 0a	0 ± 0a	0 ± 0a	0 ± 0a
Ammonia oxidation$_{max}$ (μg N kg d^{-1})	13.6 ± 3.1b	17.4 ± 3.2b	25.2 ± 0.5a	21.1 ± 5.7b	20.5 ± 6.9b	38.6 ± 6.4a*
Ammonia oxidation$_{min}$ (μg N kg d^{-1})	5.1 ± 2.4b	8.9 ± 2.1b	20.7 ± 0.9a	15.6 ± 5.4a	15.2 ± 4.5a	23.2 ± 4.7a
Nitrifier denitrification$_{max}$ (μg N kg d^{-1})	17.8 ± 2.5a	17.1 ± 3a	10.2 ± 2.5b	13.4 ± 3.5b	14.4 ± 5b	32.7 ± 3.8a*
Nitrifier denitrification$_{min}$ (μg N kg d^{-1})	3.7 ± 0.9a*	2.2 ± 0.6ab	0.9 ± 0.4b	0.4 ± 0.3b	1.4 ± 1.1ab	3.9 ± 1.6a*
Nitrification-coupled denitrification$_{max}$ (μg N kg d^{-1})	5.6 ± 0.8a	6.4 ± 1a	4.8 ± 1.7a	7.7 ± 3.8b	7.8 ± 1.6b	13.3 ± 1.3a*
Heterotrophic denitrification (μg N kg d^{-1})	3 ± 1.5b	8 ± 1.9a	5.5 ± 1.6ab	10.7 ± 2.7a	10.3 ± 2a	13.5 ± 2.3a
Gross N mineralization rate (mg N kg d^{-1})	2.5 ± 0.4b	3.4 ± 0.2a*	3.7 ± 0.2a*	3.1 ± 0.8a	2.2 ± 0.7ab	1.2 ± 0.2b
Gross nitrification rate (mg N kg d^{-1})	2.5 ± 0.7b	4 ± 0.7b	8.1 ± 1.1a	6.1 ± 0.8b*	5.5 ± 0.3b	8.1 ± 0.1a
RN_2O_{AN} (%)	1.0 ± 0.1a*	0.8 ± 0.1a	0.4 ± 0.1b	0.6 ± 0.1b	0.7 ± 0.1ab	0.8 ± 0.1a*
RN_2O_{AOmin} (%)	0.1 ± 0.1b	0.2 ± 0.0ab	0.3 ± 0.0a	0.3 ± 0.1a	0.3 ± 0.1a	0.3 ± 0.1a
RN_2O_{AOmax} (%)	0.4 ± 0.1a	0.4 ± 0.0a	0.3 ± 0.1a	0.3 ± 0.1a	0.4 ± 0.1a	0.5 ± 0.1a
RN_2O_{NDmin} (%)	0.1 ± 0.0a*	0.1 ± 0.0b	0.0 ± 0.0c	0.0 ± 0.0b	0.0 ± 0.0ab	0.0 ± 0.0a*
RN_2O_{NDmax} (%)	0.5 ± 0.1a*	0.4 ± 0.1a*	0.1 ± 0.0b*	0.2 ± 0.0b	0.3 ± 0.1b	0.4 ± 0.0a

Different letters denote significant difference at $p < 0.05$ level among different N additions for a variable from the same topographic position. * indicates a significant difference ($p < 0.05$) between the valley and slope for the same N addition. N0, N50, and N100 represent N addition levels as 0, 50, 100 kg N ha^{-1} yr^{-1}, respectively. RN_2O_{AN}, RN_2O_{NDmin}, RN_2O_{NDmax}, RN_2O_{AOmin}, and RN_2O_{AOmax} represent the fraction of N_2O produced by autotrophic nitrification, maximal and minima of ammonia oxidation, and nitrifier denitrification lost via nitrification, respectively

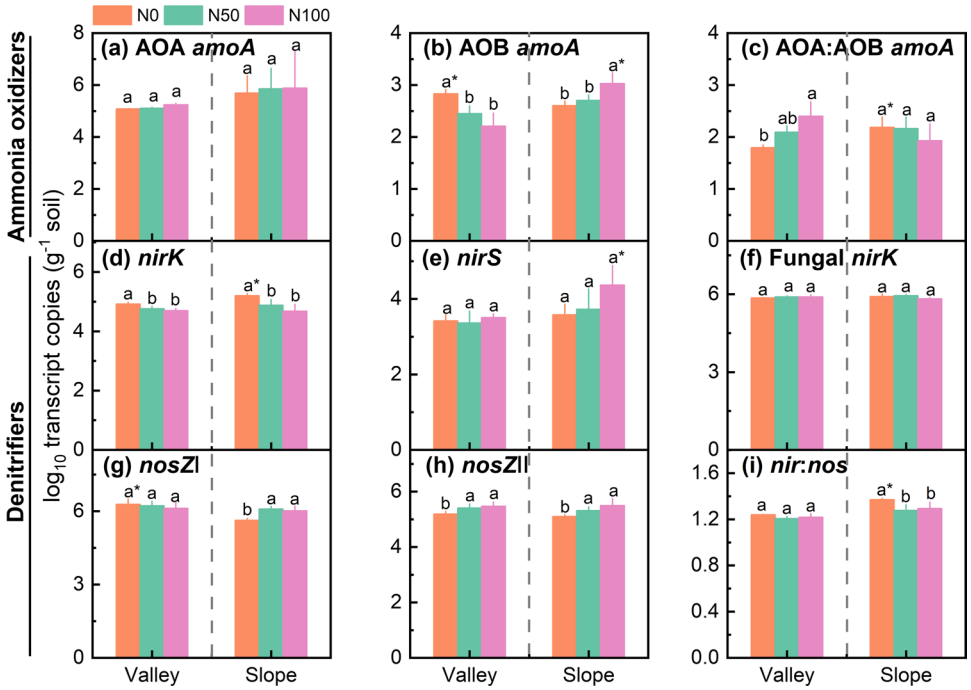

Fig. 2 Impacts of N addition on gene transcript abundances of (**a**–**c**) ammonia oxidizers and (**d**–**i**) denitrifiers in the valley and on the slope, respectively. Different letters denote significant difference at $p < 0.05$ among N addition treatments in the valley or on the slope. * represents significant difference at $p < 0.05$ between the valley and slope for the same N addition level. Values are presented as means with standard deviations ($n = 3$)

positions (Fig. 2d). Compared to control, *nosZ*I transcript was significantly ($p < 0.05$) increased on the slope, and *nosZ*II transcript was significantly ($p < 0.05$) increased at both topographic positions by chronic N addition (Fig. 2g, h). *nir:nos* ratio was significantly ($p < 0.05$) decreased by chronic N addition on the slope (Fig. 2i). *nirK* transcript and *nir:nos* ratio were significantly higher ($p < 0.05$) on the slope than in the valley, while *nosZ*I transcript was significantly higher ($p < 0.05$) in the valley than on the slope under the control (Fig. 2d, g, i). *nirS* transcript was significantly higher ($p < 0.05$) on the slope than in the valley under N100 (Fig. 2e). The transcriptional levels of *nirS* and fungal *nirK* genes were not significantly altered by N addition at both topographic positions (Fig. 2e, f).

Linking N_2O production rate from individual pathways to soil properties and gene transcript abundances

In the valley, DOC, DON, DON:AVP ratio, AOA *amoA*, and AOA:AOB *amoA* ratio were positively related to autotrophic nitrification and ammonia oxidation-derived N_2O; and NO_2^- was positively related to heterotrophic denitrification, nitrifier denitrification, and nitrification-coupled denitrification–derived N_2O (Fig. 3a). In contrast, AOB *amoA* and *nirK* transcripts were negatively related to ammonia oxidation-derived N_2O, and AOA *amoA* and *nosZ*II transcripts were negatively related to nitrifier denitrification-derived N_2O (Fig. 3a). On the slope, AVP, AOB *amoA*, and *nirS* transcripts were positively, but *nirK* transcript was negatively related to autotrophic nitrification, ammonia oxidation, and nitrifier denitrification-derived N_2O (Fig. 3b).

In the valley, SEM analysis suggested that chronic N-induced increase in soil DON and NH_4^+ concentrations indirectly increased ammonia oxidation-derived N_2O by enhancing AOA *amoA* transcript (Fig. 4). Chronic N-induced increase in soil DON:AVP ratio and decrease in soil C:N ratio indirectly decreased nitrifier denitrification-derived N_2O by inhibiting AOB *amoA* transcript. Additionally, chronic N-induced decrease in C:N ratio indirectly decreased nitrification-coupled denitrification–derived N_2O congruent with stimulated *nosZ*II transcript, and *nirS* transcript had direct effects on nitrification-coupled denitrification–derived N_2O. SEM explained 67%, 51%, and 65% of ammonia oxidation-, nitrifier denitrification- and heterotrophic denitrification-derived N_2O, respectively (Fig. 4).

On the slope, SEM analysis demonstrated that chronic N-induced increase in soil AVP indirectly increased ammonia oxidation-derived N_2O congruent with accelerated AOB *amoA* transcript. Chronic N-induced increase in soil AVP indirectly increased nitrifier denitrification-derived N_2O congruent with accelerated AOB *amoA* transcript, and chronic N addition also indirectly influenced nitrifier denitrification-derived N_2O congruent with decreased *nirK* transcript. SEM explained 78% and 79% of ammonia oxidation- and nitrifier denitrification-derived N_2O, respectively (Fig. 4).

Fig. 3 Correlations of N_2O production pathways with soil properties and functional genes transcript abundances (**a**) in the valley and (**b**) on the slope. Size and color of the circles indicate the strength and sign of the correlation. *$p<0.05$, **$p<0.01$

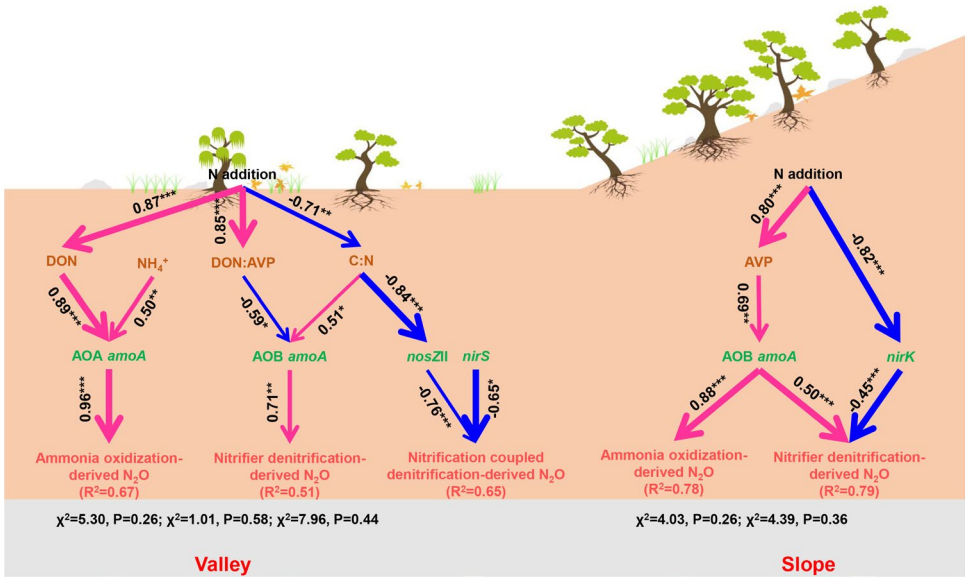

Fig. 4 Schematic illustrating mechanisms underlying the effects of N addition on the amount of N_2O derived from different biological pathways in the valley or on the slope. The blue solid lines represent significant negative relationships and the pink solid lines represent significant positive relationships. Width of arrows represents the strength of the relationships. The proportion of variance explained (R^2) appears alongside each response variable in the model. Numbers alongside arrows are standardized path coefficients with asterisks indicating their significance levels (*$p<0.05$, ** $p<0.01$, *** $p<0.001$)

Discussion

Relative contributions of individual pathways to N_2O production are topography-dependent

We find that autotrophic nitrification dominated soil N_2O production in the subtropical karst forest. This is in line with some previous studies, reinforcing that autotrophic nitrification plays a key role in soil nitrification process for karst forests with calcareous soils (Li et al. 2017; Zhu et al. 2016). Nevertheless, in some subtropical forests, heterotrophic nitrification plays a pivotal role by accounting for 30–45% of soil N_2O production (Han et al. 2018b; Zhang et al. 2018b). In these studies, low soil pH, high SOC content, and C:N ratio have been used to explain the high contribution of heterotrophic nitrification to N_2O production (Han et al. 2018b; Zhang et al. 2018b). Because SOC content and C:N ratio in the current study (Table S3) are within the range reported by Zhang et al. (2018b) and Zhu et al. (2021), we speculated that the dominance of autotrophic nitrification in N_2O production should be caused by the relatively high soil pH (7.1–7.5) (Table S3).

Our results show that the contribution of autotrophic nitrification to N_2O production was affected by topography. Low soil C:N ratio, high gross nitrification rate, and P availability have been found to stimulate the contribution of autotrophic nitrification to N_2O production (Cui et al. 2020; Duan et al. 2019c; Zhang et al. 2018a). However, soil C:N ratio was similar between the two topographic positions, and gross nitrification rate was significantly higher on the slope than in the valley in the current study (Tables 1 and S3). Thus, higher contribution of autotrophic nitrification to N_2O production in the valley may be due to the higher P level, since high P availability usually simulates AOB *amoA* abundance (Shi et al. 2018). In support of this, both soil AVP content and AOB *amoA* transcript abundance were significantly higher in the valley than on the slope (Table S3; Fig. 2b), supporting the critical role of P availability in promoting AOB activity. Additionally, the higher contribution of autotrophic nitrification to N_2O production could partly contribute to the observed higher proportion of nitrified N lost as N_2O in the valley ($p < 0.05$) (Table 1).

The present study demonstrates that the contributions of nitrifier denitrification and heterotrophic denitrification to soil N_2O production were also affected by topography (Fig. 1c). It has been reported that nitrifier denitrification would be especially favored at low oxygen, C availability, and pH conditions, and conducted only by AOB (Prommer et al. 2020; Wrage-Mönnig et al. 2018). Considering that nitrite oxidation is more sensitive to low pH than ammonia oxidation (Han et al. 2018a; Jung et al. 2019), more nitrite would be accumulated and become toxic to ammonium oxidizers and thus favor nitrifier denitrification under lower pH condition (Shi et al. 2017). Similarly, soil pH was significantly lower in the valley than on the slope in the current study (Table S3). Therefore, the higher contribution of nitrifier denitrification to N_2O production could partly be attributed to the lower pH in the valley. Concerning the influence of C availability on N_2O production (Florio et al. 2019; Hu et al. 2016), microbes can regulate their N use efficiency by releasing NH_4^+ produced by the mineralization of organic N when C is limited and immobilization of inorganic N occurs when N is limited (Mooshammer et al. 2014). Thus, C limitation would stimulate N_2O production via nitrifier denitrification pathways (Wrage-Mönnig et al. 2018; Wu et al. 2018). This is supported by the observation that the fraction of N_2O lost via nitrifier denitrification in the valley with low DOC concentration was significantly higher than that on the slope (Table 1). Higher contribution of nitrifier denitrification to N_2O production in the valley may be due to the lower DOC concentration level, since low C availability usually enhances AOB *amoA* abundace (Xiao et al. 2020). High C availability is known to lead to the establishment of anaerobic microsites due to stimulated heterotrophic microbial activity, and thus provides favorable conditions for heterotrophic denitrification (Grave et al. 2018). Therefore, higher DOC contents (Table S3) along with high *nir*:*nos* ratio (Fig. 2i) on the slope relative to the valley may partly explain the greater contribution of heterotrophic denitrification to N_2O production in the current study.

Although co-denitrification has been identified as a potential soil N_2O production pathway (Duan et al. 2019c; Harris et al. 2021; Jansen-Willems et al. 2016; Tang et al. 2018), its contribution to N_2O production was negligible in the present study (0.0–0.2%) (Fig. 1b). A possible reason for this may be the relatively low fungi abundance in alkaline soils, so that co-denitrification is not favored (Rex et al. 2019).

Nitrogen addition stimulates N_2O production rate via ammonia oxidation in the valley

We find that N addition stimulated soil N_2O production rate largely via ammonia oxidation in the valley, supporting Hypothesis I. In line with our results, several studies reported an increase in N_2O production activity from ammonia oxidation under N addition (Fu et al. 2020; Hink et al. 2018; Meinhardt et al. 2018). It was proposed that high inorganic N inputs stimulates AOB activity and their production of N_2O (Hink et al. 2018), because AOB activity is favored by high levels of NH_4^+ while AOA activity is tightly linked to organic N mineralization (Prosser et al. 2020). However, in the current study, AOB *amoA* transcript was significantly reduced by N addition in the valley (Fig. 2b), so that the stimulation of ammonia oxidation-derived N_2O by N addition might not be caused by AOB. In contrast, AOA was identified as the strongest explanatory variable for ammonia oxidation-derived N_2O in the present study (Fig. 4). The dominant role of AOA in ammonia oxidation could be due to the increase in N mineralization and thus the availability of mineralized NH_4^+ under N addition (Huang et al. 2021; Lu et al. 2015). In support of this, our data showed that AOA *amoA* transcript was positively correlated with DON (Figs. 4, S3a). Soil DON is largely produced via depolymerization of high molecular weight organic N (e.g., protein), and is the substrate of gross N mineralization, which produces NH_4^+ (Mooshammer et al. 2017). Therefore, AOA was responsible for the increased ammonia oxidation-derived N_2O due to increased N mineralization by N addition in the valley (Table 1).

Nitrogen addition stimulates N_2O production rate via ammonia oxidation and nitrifier denitrification on the slope

It has been observed in a few studies that enhanced N_2O production was related to ammonia oxidation under N addition (Duan et al. 2019c; Zhang et al. 2018a). Consistently, N addition stimulated soil N_2O production rate mainly via ammonia

oxidation on the slope in the current study, supporting Hypothesis I. Some studies show that the stimulation of ammonia oxidation under N addition was caused by directly providing NH_4^+ substrate for AOB growth (Cheng et al. 2020; Hink et al. 2018, 2017; Rütting et al. 2021; Song et al. 2021; Wang et al. 2016). However, soil NH_4^+ content was not significantly altered by N addition (Table S1), and N addition did not have a direct effect on AOB *amoA* transcript on the slope (Fig. 4), so that the enhancement in AOB activity should not be caused by direct substrate supplying under N addition. Previous studies have pointed out that AOB abundance and community composition can be more limited by P availability than AOA (Shi et al. 2018; Xiang et al. 2017; Yang et al. 2020). In the current study, a positive correlation between soil AVP content and AOB *amoA* transcript on the slope (Figs. 4, S3b) indicated that the promoted P availability contributed to the increase of AOB activity under N addition, since increasing P availability facilitates microbial growth (Bicharanloo et al. 2022). Consequently, elevated N addition would promote ammonia oxidization-derived N_2O on the slope through accelerating AOB activity (Fig. 4).

Nitrogen addition also stimulated soil N_2O production rate from nitrifier denitrification on the slope. This is consistent with the findings of some previous studies (Huang et al. 2014; Wu et al. 2018; Zhang et al. 2016). They attributed this to large NO_2^- accumulation, low C and oxygen availability, and N-induced acidity (Wrage-Mönnig et al. 2018). However, soil NO_2^- concentration, C:N ratio, C:P ratio, and pH were not significantly altered by N addition on the slope (Table S3), so that the stimulation of soil N_2O production by N addition should not be caused by these factors. In the current study, the AVP concentration, gross nitrification rate, and AOB *amoA* transcript were significantly increased by N addition on the slope. Increase in P availability may benefit adenosine triphosphate (ATP) synthesis, so that providing energy for soil AOB growth (Shi et al. 2018), which is subsequently in favor of soil nitrification (Mehnaz and Dijkstra 2016; O'Neill et al. 2021). It has been reported that the increase of nitrification would result in oxygen depletion in soil microsites (Song et al. 2022), where nitrifier denitrification would subsequently increase substantially (Zhu et al. 2013), and contribute to the observed increase of nitrifier denitrification-derived N_2O on the slope in the current study. In addition, RN_2O_{ND} was significantly increased by N addition (Table 1), so that the stimulation of soil N_2O production derived from nitrifier denitrification under N addition should be caused by enhanced gross nitrification rate on the slope.

Nitrogen addition decreases N_2O production rate via nitrifier denitrification and nitrification-coupled denitrification in the valley

The current study reveals that N addition significantly suppressed N_2O production from nitrifier denitrification and nitrification-coupled denitrification in the valley, which is in contrast to Hypothesis II. A previous study showed that nitrifier denitrification derived-N_2O was reduced under high N addition (Deppe et al. 2017), consistent with the present study. Based on the stoichiometric decomposition theory, microbes obtain resources and adjust their resource use efficiency according to their optimal stoichiometric C:N:P ratio (Sinsabaugh and Shah 2012). For example, when C:N ratio decreases, microbial C (energy) limitation would increase along with stimulated C use efficiency and N mineralization (Zechmeister-Boltenstern et al. 2015). Our results showed that N addition significantly decreased soil C:N ratio but increased DON:AVP ratio in the valley (Table S3), implying that microbes would increase N mineralization rate, which is supported by our data (Table 1). The growth of AOA has been linked to organic N mineralization with low fluxes of NH_4^+ (Prosser et al. 2020), so that AOA would outcompete AOB when soil NH_4^+ is generated by the mineralization of organic N (Hink et al. 2018). In the current study, AOB activity was significantly suppressed along with stimulated gross N mineralization under N addition (Fig. 2b, Table 1), leading to decreased contribution of nitrifier denitrification to N_2O production in the valley. Furthermore, the suppressed AOB activity would theoretically result in suppressed N_2O production via nitrification-coupled denitrification due to the reduced supply of nitrate (Shi et al. 2017). However, soil NO_3^- concentrations was significantly increased by N addition in the valley (Table S3), so that the inhibition of soil N_2O production via nitrification-coupled denitrification by N addition should not be caused by soil NO_3^-. Increase of N_2O reduction has often been used to explain the suppression of N_2O production from nitrification-coupled denitrification (Bakken and Frostegård 2017). In the current study, the transcript of the *nosZ*II, which encodes the enzyme catalyzing the reduction of N_2O to N_2 (Hallin et al. 2018), was negatively related to nitrification-coupled denitrification–derived N_2O (Fig. 4), supporting that the suppressed N_2O production from nitrification-coupled denitrification was partly explained by N_2O reduction in the valley.

Nitrogen addition decreases the relative contribution of heterotrophic denitrification to N_2O production on the slope

We find that the relative importance of heterotrophic denitrification in N_2O production decreased under N addition on the slope but not in the valley (Fig. 1b). A few previous

studies show that N addition inhibited N_2O production from heterotrophic denitrification (Peng et al. 2021; Tang et al. 2018), consistent with the present study. One possibility is that N addition may promote N_2O reduction. The important role of soil P availability on denitrification has been demonstrated in a few studies, either by enhancing N_2O reductase abundance (Ma et al. 2016; Tang et al. 2016) or via influencing soil denitrification rate (Deveautour et al. 2022). In the current study, the transcripts of *nosZ*I and *nosZ*II, which encode N_2O reductase, were found to be simulated by N addition (Fig. 2), and they were negatively correlated with DOC:AVP and DON:AVP ratios on the slope, respectively (Fig. S3b). A few studies reported that the enhanced *nosZ*I and *nosZ*II transcripts were accompanied with low N_2O production from denitrification due to promoted N_2O reduction to N_2 (Domeignoz-Horta et al. 2018; Jones et al. 2014). The above mechanism explained the observation that N addition had negative effects on the contribution of heterotrophic denitrification to N_2O production on the slope (Fig. 1b). However, we should note that the sets of primers used in the current study may not capture a broader taxonomic coverage of microbes harboring *nosZ*I gene, but a new primer set introduced by Zhang et al. (2021) may increase the coverage of N_2O reducers.

Conclusions

Our results show that autotrophic nitrification pathways were mainly responsible for soil N_2O production in a subtropical karst forest regardless of topographic position. Though N addition stimulated soil N_2O production, the pathways responsible for the stimulation were topography dependent, i.e., ammonia oxidation in the valley but ammonia oxidation and nitrifier denitrification on the slope. Nitrogen addition also suppressed the relative importance of a few pathways in soil N_2O production with the pathways being different between the two topographic positions. The differences in N transformation, N_2O production, and their responses to atmospheric N deposition among topographic positions in subtropical forests should be further explored in combination of functional microbial community composition.

Supplementary Information The online version contains supplementary material available at https://doi.org/10.1007/s00374-022-01653-w.

Funding This work was funded by the National Natural Science Foundation of China (32001175, 31760153), Guangxi Bagui Scholarship Program to Dejun Li.

Data availability The data that support the findings of this study are available upon reasonable request from the authors.

Declarations

Conflict of interest The authors declare no competing interests.

References

Aldossari N, Ishii S (2021) Fungal denitrification revisited—recent advancements and future opportunities. Soil Biol Biochem 157:108250

Arias-Navarro C, Díaz-Pinés E, Klatt S, Brandt P, Rufino MC, Butterbach-Bahl K, Verchot LV (2017) Spatial variability of soil N_2O and CO_2 fluxes in different topographic positions in a tropical montane forest in Kenya. J Geophys Res: Biogeo 122:514–527

Bakken LR, Frostegård Å (2017) Sources and sinks for N_2O, can microbiologist help to mitigate N_2O emissions? Environ Microbiol 19:4801–4805

Bicharanloo B, Bagheri Shirvan M, Keitel C, Dijkstra FA (2022) Nitrogen and phosphorus availability have stronger effects on gross and net nitrogen mineralisation than wheat rhizodeposition. Geoderma 405:115440

Brookes PC, Landman A, Pruden G, Jenkinson D (1985) Chloroform fumigation and the release of soil nitrogen: a rapid direct extraction method to measure microbial biomass nitrogen in soil. Soil Biol Biochem 17:837–842

Butterbach-Bahl K, Baggs EM, Dannenmann M, Kiese R, Zechmeisterboltenstern S (2013) Nitrous oxide emissions from soils: how well do we understand the processes and their controls? Philos T R Soc B 368:91–97

Chalk PM, Smith CJ (2020) The role of agroecosystems in chemical pathways of N_2O production. Agr Ecosyst Environ 290:106783

Chen H, Tang J, Sun X, Ma K, Chen H, Li D (2021) Topography modulates effects of nitrogen deposition on microbial resource limitation in a nitrogen-saturated subtropical forest. For Ecosyst 8:1–9

Cheng Y, Wang J, Wang J, Wang S, Chang SX, Cai Z, Zhang J, Niu S, Hu S (2020) Nitrogen deposition differentially affects soil gross nitrogen transformations in organic and mineral horizons. Earth-Sci Rev 201:103033

Clark IM, Buchkina N, Jhurreea D, Goulding KW, Hirsch PR (2012) Impacts of nitrogen application rates on the activity and diversity of denitrifying bacteria in the Broadbalk Wheat Experiment. Philos T R Soc B 367:1235–1244

Congreves KA, Phan T, Farrell RE (2019) A new look at an old concept: using $^{15}N_2O$ isotopomers to understand the relationship between soil moisture and N_2O production pathways. SOIL 5:265–274

Cui Y, Zhang Y, Duan C, Wang X, Zhang X, Ju W, Chen H, Yue S, Wang Y, Li S, Fang L (2020) Ecoenzymatic stoichiometry reveals microbial phosphorus limitation decreases the nitrogen cycling potential of soils in semi-arid agricultural ecosystems. Soil till Res 197:104463

Davidson EA, Hart SC, Shanks CA, Firestone MK (1991) Measuring gross nitrogen mineralization, immobilization, and nitrification by ^{15}N isotopic pool dilution in intact soil cores. Eur J Soil Sci 42:335–349

Deppe M, Well R, Giesemann A, Spott O, Flessa H (2017) Soil N_2O fluxes and related processes in laboratory incubations simulating ammonium fertilizer depots. Soil Biol Biochem 104:68–80

Deveautour C, Rojas-Pinzon PA, Veloso M, Rambaud J, Duff AM, Wall D, Carolan R, Philippot L, Richards KG, O'Flaherty V, Brennan F (2022) Biotic and abiotic predictors of potential N_2O emissions from denitrification in Irish grasslands soils: a national-scale field study. Soil Biol Biochem 168:108637

Domeignoz-Horta LA, Philippot L, Peyrard C, Bru D, Breuil M-C, Bizouard F, Justes E, Mary B, Léonard J, Spor A (2018) Peaks of in situ N_2O emissions are influenced by N_2O-producing and reducing microbial communities across arable soils. Global Change Biol 24:360–370

Duan P, Song Y, Li S, Xiong Z (2019a) Responses of N_2O production pathways and related functional microbes to temperature across greenhouse vegetable field soils. Geoderma 355:113904

Duan P, Zhang Q, Zhang X, Xiong Z (2019b) Mechanisms of mitigating nitrous oxide emissions from vegetable soil varied with manure, biochar and nitrification inhibitors. Agr Forest Meteorol 278:107672

Duan P, Zhou J, Feng L, Jansen-Willems AB, Xiong Z (2019c) Pathways and controls of N_2O production in greenhouse vegetable production soils. Biol Fert Soils 55:285–297

Florio A, Bréfort C, Gervaix J, Bérard A, Le Roux X (2019) The responses of NO_2^-- and N_2O-reducing bacteria to maize inoculation by the PGPR Azospirillum lipoferum CRT1 depend on carbon availability and determine soil gross and net N_2O production. Soil Biol Biochem 136:107524

Fu Z, Chen H, Xu Q, Jia J, Wang S, Wang K (2016) Role of epikarst in near-surface hydrological processes in a soil mantled subtropical dolomite karst slope: implications of field rainfall simulation experiments. Hydrol Process 30:795–811

Fu Q, Xi R, Zhu J, Hu H, Xing Z, Zuo J (2020) The relative contribution of ammonia oxidizing bacteria and archaea to N_2O emission from two paddy soils with different fertilizer N sources: a microcosm study. Geoderma 375:114486

Grave RA, Nicoloso RdS, Cassol PC, da Silva MLB, Mezzari MP, Aita C, Wuaden CR (2018) Determining the effects of tillage and nitrogen sources on soil N_2O emission. Soil till Res 175:1–12

Carter MR, Gregorich EG (eds) (2007) Soil sampling and methods of analysis, 2nd edn. CRC Press. https://doi.org/10.1201/9781420005271

Hallin S, Philippot L, Löffler FE, Sanford RA, Jones CM (2018) Genomics and ecology of novel N_2O-reducing microorganisms. Trends Microbiol 26:43–55

Han S, Zeng L, Luo X, Xiong X, Wen S, Wang B, Chen W, Huang Q (2018a) Shifts in *Nitrobacter*- and *Nitrospira*-like nitrite-oxidizing bacterial communities under long-term fertilization practices. Soil Biol Biochem 124:118–125

Han X, Shen W, Zhang J, Müller C (2018b) Microbial adaptation to long-term N supply prevents large responses in N dynamics and N losses of a subtropical forest. Sci Total Environ 626:1175–1187

Han X, Xu C, Nie Y, He J, Wang W, Deng Q, Shen W (2019) Seasonal variations in N_2O emissions in a subtropical forest with exogenous nitrogen enrichment are predominately influenced by the abundances of soil nitrifiers and denitrifiers. Biogeosciences 124:3635–3651

Hao T, Zhang Y, Zhang J, Müller C, Li K, Zhang K, Chu H, Stevens C, Liu X (2020) Chronic nitrogen addition differentially affects gross nitrogen transformations in alpine and temperate grassland soils. Soil Biol Biochem 149:107962

Harris E, Diaz-Pines E, Stoll E, Schloter M, Schulz S, Duffner C, Li K, Moore KL, Ingrisch J, Reinthaler D, Zechmeister-Boltenstern S, Glatzel S, Brüggemann N, Bahn M (2021) Denitrifying pathways dominate nitrous oxide emissions from managed grassland during drought and rewetting. Sci Adv 7: eabb7118

Hink L, Nicol GW, Prosser JI (2017) Archaea produce lower yields of N_2O than bacteria during aerobic ammonia oxidation in soil. Environ Microbiol 19:4829–4837

Hink L, Gubry-Rangin C, Nicol GW, Prosser JI (2018) The consequences of niche and physiological differentiation of archaeal and bacterial ammonia oxidisers for nitrous oxide emissions. ISME J 12:1084–1093

Hu X, Liu L, Zhu B, Du E, Hu X, Li P, Zhou Z, Ji C, Zhu J, Shen H, Fang J (2016) Asynchronous responses of soil carbon dioxide, nitrous oxide emissions and net nitrogen mineralization to enhanced fine root input. Soil Biol Biochem 92:67–78

Huang T, Gao B, Hu X-K, Lu X, Well R, Christie P, Bakken LR, Ju X-T (2014) Ammonia-oxidation as an engine to generate nitrous oxide in an intensively managed calcareous Fluvo-aquic soil. Sci Rep 4:1–9

Huang L, Chakrabarti S, Cooper J, Perez A, John SM, Daroub SH, Martens-Habbena W (2021) Ammonia-oxidizing archaea are integral to nitrogen cycling in a highly fertile agricultural soil. ISME Commun 1:19

Jansen-Willems AB, Lanigan GJ, Clough TJ, Andresen LC, Müller C (2016) Long-term elevation of temperature affects organic N turnover and associated N_2O emissions in a permanent grassland soil. SOIL 2:601–614

Jones CM, Spor A, Brennan FP, Breuil M-C, Bru D, Lemanceau P, Griffiths B, Hallin S, Philippot L (2014) Recently identified microbial guild mediates soil N_2O sink capacity. Nat Clim Change 4:801–805

Jung MY, Gwak JH, Rohe L, Giesemann A, Kim JG, Well R, Madsen EL, Herbold CW, Wagner M, Rhee SK (2019) Indications for enzymatic denitrification to N_2O at low pH in an ammonia-oxidizing archaeon. ISME J 13:2633–2638

Kool DM, Dolfing J, Wrage N, Van Groenigen JW (2011) Nitrifier denitrification as a distinct and significant source of nitrous oxide from soil. Soil Biol Biochem 43:174–178

Krause H-M, Thonar C, Eschenbach W, Well R, Mäder P, Behrens S, Kappler A, Gattinger A (2017) Long term farming systems affect soils potential for N_2O production and reduction processes under denitrifying conditions. Soil Biol Biochem 114:31–41

Laughlin RJ, Stevens RJ, Zhuo S (1997) Determining nitrogen-15 in ammonium by producing nitrous oxide. Soil Sci Soc Am J 61:462–465

Li D, Yang Y, Chen H, Xiao K, Song T, Wang K (2017) Soil gross nitrogen transformations in typical karst and nonkarst forests, Southwest China. J Geophys Res: Biogeo 122:2831–2840

Li D, Liu J, Chen H, Zheng L, Wang K (2018) Soil gross nitrogen transformations in responses to land use conversion in a subtropical karst region. J Environ Manage 212:1–7

Li C, He ZY, Hu HW, He JZ (2022) Niche specialization of comammox Nitrospira in terrestrial ecosystems: oligotrophic or copiotrophic? Crit Rev Env Sci Tech: 1–16. https://doi.org/10.1080/10643389.2022.2049578

Liu D, Fang Y, Tu Y, Pan Y (2014) Chemical method for nitrogen isotopic analysis of ammonium at natural abundance. Anal Chem 86:3787–3792

Lu X, Bottomley PJ, Myrold DD (2015) Contributions of ammonia-oxidizing archaea and bacteria to nitrification in Oregon forest soils. Soil Biol Biochem 85:54–62

Ma W, Jiang S, Assemien F, Qin M, Ma B, Xie Z, Liu Y, Feng H, Du G, Ma X (2016) Response of microbial functional groups involved in soil N cycle to N, P and NP fertilization in Tibetan alpine meadows. Soil Biol Biochem 101:195–206

Mehnaz KR, Dijkstra FA (2016) Denitrification and associated N_2O emissions are limited by phosphorus availability in a grassland soil. Geoderma 284:34–41

Meinhardt KA, Stopnisek N, Pannu MW, Strand SE, Fransen SC, Casciotti KL, Stahl DA (2018) Ammonia-oxidizing bacteria are the primary N_2O producers in an ammonia-oxidizing archaea dominated alkaline agricultural soil. Environ Microbiol 20:2195–2206

Montzka SA, Dlugokencky EJ, Butler JH (2011) Non-CO_2 greenhouse gases and climate change. Nature 476:43–50

Mooshammer M, Wanek W, Hämmerle I, Fuchslueger L, Hofhansl F, Knoltsch A, Schnecker J, Takriti M, Watzka M, Wild B (2014)

Adjustment of microbial nitrogen use efficiency to carbon: nitrogen imbalances regulates soil nitrogen cycling. Nat Commun 5:1–7

Mooshammer M, Hofhansl F, Frank AH, Wanek W, Hämmerle I, Leitner S, Schnecker J, Wild B, Watzka M, Keiblinger KM, Zechmeister-Boltenstern S, Richter A (2017) Decoupling of microbial carbon, nitrogen, and phosphorus cycling in response to extreme temperature events. Sci Adv 3:e1602781

O'Neill RM, Krol DJ, Wall D, Lanigan GJ, Renou-Wilson F, Richards KG, Jansen-Willems AB, Müller C (2021) Assessing the impact of long-term soil phosphorus on N-transformation pathways using ^{15}N tracing. Soil Biol Biochem 152:108066

Parton W, Mosier A, Ojima D, Valentine D, Schimel D, Weier K, Kulmala AE (1996) Generalized model for N_2 and N_2O production from nitrification and denitrification. Global Biogeochem Cy 10:401–412

Peng B, Sun J, Liu J, Xia Z, Dai W (2021) Relative contributions of different substrates to soil N_2O emission and their responses to N addition in a temperate forest. Sci Total Environ 767:144126

Prommer J, Walker TWN, Wanek W, Braun J, Zezula D, Hu Y, Hofhansl F, Richter A (2020) Increased microbial growth, biomass, and turnover drive soil organic carbon accumulation at higher plant diversity. Global Change Biol 26:669–681

Prosser JI, Hink L, Gubry-Rangin C, Nicol GW (2020) Nitrous oxide production by ammonia oxidizers: physiological diversity, niche differentiation and potential mitigation strategies. Global Change Biol 26:103–118

Rex D, Clough TJ, Richards KG, Condron LM, de Klein CAM, Morales SE, Lanigan GJ (2019) Impact of nitrogen compounds on fungal and bacterial contributions to codenitrification in a pasture soil. Sci Rep 9:13371

Rütting T, Schleusner P, Hink L, Prosser JI (2021) The contribution of ammonia-oxidizing archaea and bacteria to gross nitrification under different substrate availability. Soil Biol Biochem 160:108353

Sexstone AJ, Revsbech NP, Parkin TB, Tiedje JM (1985) Direct measurement of oxygen profiles and denitrification rates in soil aggregates. Soil Sci Soc Am J 49:645–651

Shi X, Hu HW, Zhu-Barker X, Hayden H, Wang J, Suter H, Chen D, He JZ (2017) Nitrifier-induced denitrification is an important source of soil nitrous oxide and can be inhibited by a nitrification inhibitor 3,4-dimethylpyrazole phosphate. Environ Microbiol 19:4851–4865

Shi X, Hu HW, Wang J, He JZ, Zheng C, Wan X, Huang Z (2018) Niche separation of comammox *Nitrospira* and canonical ammonia oxidizers in an acidic subtropical forest soil under long-term nitrogen deposition. Soil Biol Biochem 126:114–122

Sinsabaugh RL, Shah JJF (2012) Ecoenzymatic stoichiometry and ecological theory. Annu Rev Ecol Evol S 43:313–343

Song L, Drewer J, Zhu B, Zhou M, Cowan N, Levy P, Skiba U (2020) The impact of atmospheric N deposition and N fertilizer type on soil nitric oxide and nitrous oxide fluxes from agricultural and forest Eutric Regosols. Biol Fert Soils 56:1077–1090

Song X, Wei H, Rees RM, Ju X (2022) Soil oxygen depletion and corresponding nitrous oxide production at hot moments in an agricultural soil. Environ Pollut 292:118345

Song L, Li Z, Niu S (2021) Global soil gross nitrogen transformation under increasing nitrogen deposition. Global Biogeochem Cy 35: e2020GB006711

Soper FM, Sullivan BW, Nasto MK, Osborne BB, Bru D, Balzotti CS, Taylor PG, Asner GP, Townsend AR, Philippot L, Porder S, Cleveland CC (2018) Remotely sensed canopy nitrogen correlates with nitrous oxide emissions in a lowland tropical rainforest. Ecology 99:2080–2089

Spott O, Russow R, Stange CF (2011) Formation of hybrid N_2O and hybrid N_2 due to codenitrification: first review of a barely considered process of microbially mediated N-nitrosation. Soil Biol Biochem 43:1995–2011

Stevens RJ, Laughlin RJ (1994) Determining nitrogen-15 in nitrite or nitrate by producing nitrous oxide. Soil Sci Soc Am J 58:1108–1116

Stewart KJ, Grogan P, Coxson DS, Siciliano SD (2014) Topography as a key factor driving atmospheric nitrogen exchanges in arctic terrestrial ecosystems. Soil Biol Biochem 70:96–112

Tang Y, Zhang X, Li D, Wang H, Chen F, Fu X, Fang X, Sun X, Yu G (2016) Impacts of nitrogen and phosphorus additions on the abundance and community structure of ammonia oxidizers and denitrifying bacteria in Chinese fir plantations. Soil Biol Biochem 103:284–293

Tang W, Chen D, Phillips OL, Liu X, Zhou Z, Li Y, Xi D, Zhu F, Fang J, Zhang L, Lin M, Wu J, Fang Y (2018) Effects of long-term increased N deposition on tropical montane forest soil N_2 and N_2O emissions. Soil Biol Biochem 126:194–203

Tian H, Yang J, Xu R, Lu C, Canadell JG, Davidson EA, Jackson RB, Arneth A, Chang J, Ciais P, Gerber S, Ito A, Joos F, Lienert S, Messina P, Olin S, Pan S, Peng C, Saikawa E, Thompson RL, Vuichard N, Winiwarter W, Zaehle S, Zhang B (2019a) Global soil nitrous oxide emissions since the preindustrial era estimated by an ensemble of terrestrial biosphere models: magnitude, attribution, and uncertainty. Global Change Biol 25:640–659

Tian J, Dungait JAJ, Lu X, Yang Y, Hartley IP, Zhang W, Mo J, Yu G, Zhou J, Kuzyakov Y (2019b) Long-term nitrogen addition modifies microbial composition and functions for slow carbon cycling and increased sequestration in tropical forest soil. Global Change Biol 25:3267–3281

Tian H, Xu R, Canadell JG, Thompson RL, Winiwarter W, Suntharalingam P, Davidson EA, Ciais P, Jackson RB, Janssens-Maenhout G, Prather MJ, Regnier P, Pan N, Pan S, Peters GP, Shi H, Tubiello FN, Zaehle S, Zhou F, Arneth A, Battaglia G, Berthet S, Bopp L, Bouwman AF, Buitenhuis ET, Chang J, Chipperfield MP, Dangal SRS, Dlugokencky E, Elkins JW, Eyre BD, Fu B, Hall B, Ito A, Joos F, Krummel PB, Landolfi A, Laruelle GG, Lauerwald R, Li W, Lienert S, Maavara T, MacLeod M, Millet DB, Olin S, Patra PK, Prinn RG, Raymond PA, Ruiz DJ, van der Werf GR, Vuichard N, Wang J, Weiss RF, Wells KC, Wilson C, Yang J, Yao Y (2020) A comprehensive quantification of global nitrous oxide sources and sinks. Nature 586:248–256

Vance E, Brookes P, Jenkinson D (1987) An extraction method for measuring soil microbial biomass C. Soil Biol Biochem 19:703–707

Verhoeven E, Decock C, Barthel M, Bertora C, Sacco D, Romani M, Sleutel S, Six J (2018) Nitrification and coupled nitrification-denitrification at shallow depths are responsible for early season N_2O emissions under alternate wetting and drying management in an Italian rice paddy system. Soil Biol Biochem 120:58–69

Wang Q, Zhang LM, Shen JP, Du S, Han LL, He JZ (2016) Nitrogen fertiliser-induced changes in N_2O emissions are attributed more to ammonia-oxidising bacteria rather than archaea as revealed using 1-octyne and acetylene inhibitors in two arable soils. Biol Fert Soils 52:1163–1171

Wang Z, Li D, Zheng M, Chen H, Sun X, Wang K (2019) Topography modulates effects of nitrogen deposition on asymbiotic N_2 fixation in soil but not litter or moss in a secondary karst forest. J Geophys Res: Biogeo 124:3015–3023

Wen Z, Xu W, Li Q, Han M, Tang A, Zhang Y, Luo X, Shen J, Wang W, Li K, Pan Y, Zhang L, Li W, Collett JL, Zhong B, Wang X, Goulding K, Zhang F, Liu X (2020) Changes of nitrogen deposition in China from 1980 to 2018. Environ Inte 144:106022

Wrage-Mönnig N, Horn MA, Well R, Müller C, Velthof G, Oenema O (2018) The role of nitrifier denitrification in the production of nitrous oxide revisited. Soil Biol Biochem 123:3–16

Wu D, Zhao Z, Han X, Meng F, Wu W, Zhou M, Brüggemann N, Bol R (2018) Potential dual effect of nitrification inhibitor 3,4-dimethylpyrazole phosphate on nitrifier denitrification in the mitigation of peak N_2O emission events in North China Plain cropping systems. Soil Biol Biochem 121:147–153

Wu X, Wang F, Li T, Fu B, Lv Y, Liu G (2020) Nitrogen additions increase N_2O emissions but reduce soil respiration and CH_4 uptake during freeze–thaw cycles in an alpine meadow. Geoderma 363:114157

Xiang X, He D, He J-S, Myrold DD, Chu H (2017) Ammonia-oxidizing bacteria rather than archaea respond to short-term urea amendment in an alpine grassland. Soil Biol Biochem 107:218–225

Xiao R, Qiu Y, Tao J, Zhang X, Chen H, Reberg-Horton SC, Shi W, Shew HD, Zhang Y, Hu S (2020) Biological controls over the abundances of terrestrial ammonia oxidizers. Global Ecol Biogeogr 29:384–399

Yan Y, Ganjurjav H, Hu G, Liang Y, Li Y, He S, Danjiu L, Yang J, Gao Q (2018) Nitrogen deposition induced significant increase of N_2O emissions in an dry alpine meadow on the central Qinghai-Tibetan Plateau. Agr Ecosyst Environ 265:45–53

Yang WH, McDowell AC, Brooks PD, Silver WL (2014) New high precision approach for measuring ^{15}N–N_2 gas fluxes from terrestrial ecosystems. Soil Biol Biochem 69:234–241

Yang K, Luo S, Hu L, Chen B, Xie Z, Ma B, Ma W, Du G, Ma X, Le Roux X (2020) Responses of soil ammonia-oxidizing bacteria and archaea diversity to N, P and NP fertilization: relationships with soil environmental variables and plant community diversity. Soil Biol Biochem 145:107795

Zechmeister-Boltenstern S, Keiblinger KM, Mooshammer M, Peñuelas J, Richter A, Sardans J, Wanek W (2015) The application of ecological stoichiometry to plant–microbial–soil organic matter transformations. Ecol Monogr 85:133–155

Zhang J, Müller C, Cai Z (2015) Heterotrophic nitrification of organic N and its contribution to nitrous oxide emissions in soils. Soil Biol Biochem 84:199–209

Zhang W, Li Y, Xu C, Li Q, Lin W (2016) Isotope signatures of N_2O emitted from vegetable soil: ammonia oxidation drives N_2O production in NH_4^+-fertilized soil of North China. Sci Rep 6:29257

Zhang Y, Ding H, Zheng X, Ren X, Cardenas L, Carswell A, Misselbrook T (2018a) Land-use type affects N_2O production pathways in subtropical acidic soils. Environ Pollut 237:237–243

Zhang Y, Zhao W, Cai Z, Müller C, Zhang J (2018b) Heterotrophic nitrification is responsible for large rates of N_2O emission from subtropical acid forest soil in China. Eur J Soil Sci 69:646–654

Zhang B, Penton CR, Yu Z, Xue C, Chen Q, Chen Z, Yan C, Zhang Q, Zhao M, Quensen JF, Tiedje JM (2021) A new primer set for Clade I nosZ that recovers genes from a broader range of taxa. Biol Fert Soils 57:523–531

Zheng L, Chen H, Wang Y, Mao Q, Zheng M, Su Y, Xiao K, Wang K, Li D (2020) Responses of soil microbial resource limitation to multiple fertilization strategies. Soil till Res 196:104474

Zhu X, Burger M, Doane TA, Horwath WR (2013) Ammonia oxidation pathways and nitrifier denitrification are significant sources of N_2O and NO under low oxygen availability. P Natl Acad Sci 110:6328–6333

Zhu J, He N, Wang Q, Yuan G, Wen D, Yu G, Jia Y (2015) The composition, spatial patterns, and influencing factors of atmospheric wet nitrogen deposition in Chinese terrestrial ecosystems. Sci Total Environ 511:777–785

Zhu T, Zeng S, Qin H, Zhou K, Yang H, Lan F, Huang F, Cao J, Müller C (2016) Low nitrate retention capacity in calcareous soil under woodland in the karst region of southwestern China. Soil Biol Biochem 97:99–101

Zhu J, Jansen-Willems A, Müller C, Dörsch P (2021) Topographic differences in nitrogen cycling mediate nitrogen retention in a subtropical, N-Saturated Forest Catchment. Soil Biol Biochem 159:108303